24PM1E-01

On the Relevance of Two-Dimensional Sources for Modelling Optical Emission from Layered Media

Ariel Epstein*, Nir Tessler, Pinchas D. Einziger

Department of Electrical Engineering, Technion - Israel Institute of Technology
Haifa 32000, Israel
*arielep@tx.technion.ac.il

***Abstract*—We present analytical closed-form expressions for the radiation patterns of 2D line sources and 3D point dipoles embedded in a general multi-layered configuration. While the former are simplified model sources, used as a preliminary analytical step to reduce derivation complexity, the latter have been shown experimentally to reproduce the electromagnetic behaviour of elementary (molecular) optical sources. By decomposing the sources to current elements generating pure transverse electric (TE) or transverse magnetic (TM) polarized radiation, we arrive at a unified format for the radiation pattern expression for all sources. Analyzing the common 1D Green's function, we show that the normalized TE-polarized emission of the model 2D electric line sources reproduces *exactly* the TE-polarized radiation of molecular (3D) dipoles, and discuss the relations between the TM-polarized emission of the two species. These results specify the precise relations between the 2D and 3D models, thus providing intuition as well as guidelines for proper usage of simplified 2D results for analysis of realistic 3D optical systems.**

I. Introduction

Impulsive 2D (line) sources are used routinely in analyses of electromagnetic configurations with an invariant cross-section along one or more axes [1], [2]. Conducting such analyses is beneficial, as they allow to probe the response of a complex system to a localized excitation, while simplifying the formal derivation thanks to the reduced number of dimensions. However, the capability of 2D sources to model realistic sources in physical scenarios is not obvious. While in the radio or microwave frequencies it may be possible to construct coherent current oscillations over distances much larger than the wavelength, in the optical regime, radiation usually originates from excited molecular dipoles, which generally span over no more than tenth the wavelength and are very hard to correlate. Thus, in general, optical sources cannot be treated as line sources.

In fact, as far as electromagnetic fields are considered, these elementary sources, known as excitons, were shown to be modelled well by (3D) electric point dipoles aligned in the direction of the molecular dipoles [3]. More recently, in the frame of the extensive research of organic light-emitting diodes (OLEDs), this 3D model for elementary optical sources has been utilized and verified repeatedly for plane-stratified configurations [4], [5]. In recent work, in order to provide insight for optical optimization of these novel devices, we have derived closed-form analytical expressions for the optical emission of prototypical plane-parallel OLEDs [6]. This allowed the identification of dominant optical processes, as well as the establishment of efficient analytical engineering tools, e.g. to recover the electrical properties of the device from its radiation pattern [7]. In accordance with common practice, in order to reduce the formulation complexity while retaining the principal physical intuition, we have used 2D electric and magnetic line sources to model the excitons, rather than the more realistic 3D model of electric point dipoles. Such methodology, however, raises questions regarding the validity of the results to the physical scenario.

In this paper we demonstrate the close relations between the radiation of 2D (line) and 3D (point) sources embedded in stratified media, originating in a common 1D Green's function. By decomposing the point dipoles into current elements generating either transverse electric (TE) or transverse magnetic (TM) fields [8], [9] we formulate exact relations between the polarized emission of the 2D and 3D sources. These, in turn, shed light on the physical role of the two classes of sources, as well as establish a path for quantitative analysis of 3D systems using 2D sources, which allow simplified mathematical derivation. Importantly, these relations indicate that, by considering the incoherent nature of optical sources and their random in-plane alignment, properly interpreted 2D models are capable of *exactly* reproducing measured results, as we have already observed in previous work [7].

II. Theory

A. Formulation

We consider a plane-stratified structure of $M+N+2$ layers, with a 2D (line) or 3D (point) source embedded at a certain plane $z=z'$, sandwiched between layer (-1) and $(+1)$ (Fig. 1). The interpretation of the various parameters is conventional, and is given in great detail in [6]. For completeness we note that all sources are assumed to be time-harmonic, with time dependence of $e^{j\omega t}$; the wavenumber and wave impedance of the n-th layer are defined as $k_n = \omega\sqrt{\mu_n\varepsilon_n\left[1-j\sigma_n/\left(\omega\varepsilon_n\right)\right]}$ and $Z_n = \omega\mu_n/k_n = \left(Y_n\right)^{-1}$, where the radiation condition requires $\Im\left\{k_n\right\} \leq 0$. The observation point is denoted by $\vec{r}$, where for the 3D model $\vec{r}=\rho\cos\varphi\hat{x}+\rho\sin\varphi\hat{y}+z\hat{z}$, with (ρ,φ,z) being the cylindrical coordinate system, and for the 2D model $\vec{r}=\rho_t\hat{\rho}_t+z\hat{z}$, with the transverse coordinate varying due to the different orientation of the 2D electric (${}^e\rho_t=y$) and magnetic (${}^m\rho_t=x$) line sources [6]. In both 2D and 3D cases, the angle between the z-axis and $\vec{r}$ is θ, and the source vector is $\vec{r}\,'=z'\hat{z}$.

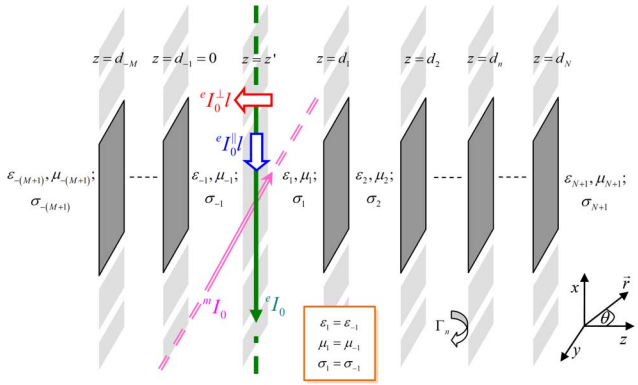

Fig. 1. Physical configuration of general stratified media with 2D electric (green solid arrow) and magnetic (magenta striped arrow) line sources, carrying currents of ${}^eI_0$ and ${}^mI_0$, respectively, and 3D electric vertical (red hollow arrow) and horizontal (blue hollow arrow) point dipoles, with dipole moments ${}^eI_0^{\perp}l$ and ${}^eI_0^{\parallel}l$, respectively. See [6] for detailed description.

As has been shown by many authors before (e.g., [1], [2], [10]) the electric and magnetic line sources (ELS and MLS), denoted here by e and m left superscripts, generate only pure TE or TM fields with respect to the z-axis, respectively; the vertical electric dipole (VED), denoted by $\perp$ superscript, generates pure TM fields, denoted by M left superscripts; and the horizontal electric dipole (HED), denoted by $\parallel$ superscript, generates both TE and TM fields, denoted by E and M left superscripts, respectively. To allow clear observation of these two HED contributions, we utilize, relying on the proof by Lindell [8], a decomposition of the HED current source, $\vec{J}^{\parallel}=-{}^eI_0 l\delta^3\left(\vec{r}-\vec{r}'\right)\hat{x}$, to two parts, ${}^E\vec{J}^{\parallel}$ and ${}^M\vec{J}^{\parallel}$, each induces only TE or TM fields with respect to the z-axis, as suggested by Sokolik *et al.* [9].

The current distributions of the various sources, corresponding to Fig. 1, are summarized in Table I. It is worth noting that as every arbitrarily oriented electric dipole can be represented by a combination of VED and HED according to its projection on the z-axis [10], our independent treatment of the VED and HED actually covers all possible dipole orientations. As for the HED current elements, one can readily verify that $\vec{J}^{\parallel}={}^E\vec{J}^{\parallel}+{}^M\vec{J}^{\parallel}$, and confirm, upon substitution of the following integral identities [11] in the definitions of Table I,

$$\frac{\delta(\rho)}{\rho}=\int_0^{\infty}k_tJ_0\left(k_t\rho\right)dk_t,\quad \frac{u(\rho)}{\rho}=\int_0^{\infty}J_1\left(k_t\rho\right)dk_t \tag{1}$$

that indeed ${}^EE_z^{\parallel}=0$ and ${}^MH_z^{\parallel}=0$, as required. In (1), $J_\nu\left(\Omega\right)$ is the νth order Bessel function of the first kind, and $u\left(\rho\right)$ is the Heaviside unit step function.

B. Green's functions

Extending previous work [6], [9], we express the transverse electromagnetic fields of the 2D and 3D cases by the 2D and 3D Green's functions, $G_2\left(\vec{r},\vec{r}'\right)$ and $G_3\left(\vec{r},\vec{r}'\right)$, satisfying the 2D and 3D Helmholtz (wave) equation in each layer, respectively (Table I). The 1D Green's function, $g(z,z')$, in turn, is defined via the spectral representation of these Green's functions, corresponding to the Fourier or Hankel transforms. These definitions imply that $g(z,z')$ satisfies the 1D Helmholtz equation at the nth layer, namely, $\left(\partial^2/\partial z^2+\beta_n^2\right)g_n(z,z')=-\delta\left(z-z'\right)$, where k_t is the transverse wavenumber and $\beta_n=\sqrt{k_n^2-k_t^2}$ is the wavenumber in the propagation direction; $g_n(z,z')$ denotes $g(z,z')$ in the nth layer.

While the transverse fields for the ELS, MLS and VED in Table I are expressed in a familiar transmission-line notion, the expressions for the HED contain the operators $\bar{\bar{I}}$ and $\bar{\bar{M}}$. These operators act on an arbitrary function $f\left(\rho\right)$, and defined as $\bar{\bar{I}}f\left(\rho\right)=f\left(\rho\right)$, $\bar{\bar{M}}f\left(\rho\right)=f\left(\rho\right)-\frac{2}{\rho^2}\int_0^{\rho}\tilde{\rho}f\left(\tilde{\rho}\right)d\tilde{\rho}$ [9].

Applying the continuity, source and radiation conditions on the 1D Green's function, we derive recursive relations for $g(z,z')$ in the various layers [2], [6]. As a matter of fact, the latter takes the same form for all sources discussed herein. For $z>z'$, or $n>0$

$$\begin{aligned}g_n(z,z')&=\frac{e^{j\beta_1z'}}{2j\beta_n}\cdot\\&\cdot\frac{1-\widehat{R}_{-1}(k_t)\,e^{-2j\beta_1z'}}{1-R_1(k_t)\,\widehat{R}_{-1}(k_t)}\left[\prod_{p=2}^{n}T_p(k_t)\right]\left[e^{-j\beta_nz}-R_n(k_t)\,e^{j\beta_nz}\right]\end{aligned} \tag{2}$$

where $R_n(k_t)$ and $T_n(k_t)$ are the total reflection and total transmission coefficients, respectively, in the forward direction, i.e., for $n>0$ [6]. These coefficients are recursively defined via

$$\begin{aligned}R_n(k_t)&=\left\{\Gamma_n(k_t)+\frac{\left[1-\Gamma_n^2(k_t)\right]R_{n+1}(k_t)\,e^{2j\beta_{n+1}d_n}}{1+\Gamma_n(k_t)R_{n+1}(k_t)\,e^{2j\beta_{n+1}d_n}}\right\}e^{-2j\beta_nd_n}\\T_n(k_t)&=\frac{\left[1+\Gamma_{n-1}(k_t)\right]e^{j(\beta_n-\beta_{n-1})d_{n-1}}}{1+\Gamma_{n-1}(k_t)R_n(k_t)\,e^{2j\beta_nd_{n-1}}}\end{aligned} \tag{3}$$

where $\Gamma_n(k_t)$ is the forward local reflection coefficient of the n-th interface, given by the Fresnel formula, $\Gamma_n=\left(1-\gamma_n\right)/\left(1+\gamma_n\right)$. The differences between the 1D Green's functions of the various sources stem from these local reflection coefficients, derived from the different continuity conditions. These are expressed by the definitions of the generalized impedance ratio, γ_n,

$${}^e_m\gamma_n=\frac{k_{n+1}\beta_n}{k_n\beta_{n+1}}\left(\frac{Z_{n+1}}{Z_n}\right)^{\pm1},\quad {}^M\gamma_n^{\perp}={}^m\gamma_n,\quad {}^E_M\gamma_n^{\parallel}=\left({}^e_m\gamma_n\right)^{\pm1} \tag{4}$$

from which simple relations between the local reflection coefficients of the 2D and 3D models can be inferred

$${}^M\Gamma_n^{\perp}={}^m\Gamma_n,\quad {}^E\Gamma_n^{\parallel}={}^e\Gamma_n,\quad {}^M\Gamma_n^{\parallel}=-{}^m\Gamma_n \tag{5}$$

The analogous expressions for the reflection and transmission coefficients in the reversed direction, $\widehat{R}_n(k_t)$, $\widehat{T}_n(k_t)$, etc., for $n<0$, can be readily derived using very simple substitutions in (3)-(5), as detailed in [6].

C. Radiation pattern

The radiation pattern is defined by the projection of the Poynting vector on the radial direction at a distant observation point,

$$S_r(\theta,\varphi)=\lim_{r\to\infty}\frac{1}{2}\left[\vec{E}\left(\vec{r},\vec{r}'\right)\times\vec{H}^*\left(\vec{r},\vec{r}'\right)\right]\cdot\hat{r} \tag{6}$$

TABLE I
2D AND 3D CURRENT SOURCES, GREEN'S FUNCTIONS AND TRANSVERSE FIELDS IN THE nTH LAYER

	2D Sources		3D Sources	
	${}^{e}I_0$ (ELS)	${}^{m}I_0$ (MLS)	${}^{e}I_0^{\perp} l$ (VED)	${}^{e}I_0^{\parallel} l$ (HED)
Current Source	${}^{e}_{m}\vec{J} = -{}^{e}_{m}I_0 \delta^2(\vec{r}-\vec{r}\,')\,\hat{\vec{x}}_{\hat{y}}$		${}^{M}\vec{J}^{\perp} = -{}^{e}I_0^{\perp} l \delta^3(\vec{r}-\vec{r}\,')\,\hat{z}$	${}^{E}_{M}\vec{J}^{\parallel} = -\frac{1}{2}{}^{e}I_0^{\parallel} l \frac{\delta(z-z')}{2\pi\rho} \begin{Bmatrix} \hat{\rho}\cos\varphi\left[(1\mp1)\,\delta(\rho) \pm \frac{u(\rho)}{\rho}\right] \\ -\hat{\varphi}\sin\varphi\left[(1\pm1)\,\delta(\rho) \mp \frac{u(\rho)}{\rho}\right] \end{Bmatrix}$
Wave Equation	$\left(\nabla^2 + k_n^2\right) G_2(\vec{r},\vec{r}\,') = -\delta^2(\vec{r}-\vec{r}\,')$		$\left(\nabla^2 + k_n^2\right) G_3(\vec{r},\vec{r}\,') = -\delta^3(\vec{r}-\vec{r}\,')$	
Spectral Integral	$G_2(\vec{r},\vec{r}\,') = \frac{1}{2\pi}\int_{-\infty}^{\infty} g(z,z')\, e^{jk_t\rho_t} dk_t$		$G_3(\vec{r},\vec{r}\,') = \frac{1}{2\pi}\int_{0}^{\infty} k_t J_0(k_t\rho)\, g(z,z')\, dk_t$	
Transverse Fields	$\begin{cases} E_x = jk_n Z_n {}^{e}I_0 G_2 \\ H_y = -{}^{e}I_0 \frac{\partial}{\partial z} G_2 \\ H_x = E_y = 0 \end{cases}$	$\begin{cases} E_x = -{}^{m}I_0 \frac{\partial}{\partial z} G_2 \\ H_y = jk_n Y_n {}^{m}I_0 G_2 \\ H_x = E_y = 0 \end{cases}$	$\begin{cases} E_\rho = -\frac{{}^{e}I_0^{\perp} l}{jk_1 Y_1} \frac{\partial^2}{\partial z \partial \rho} G_3 \\ H_\varphi = jk_n Y_n \frac{{}^{e}I_0^{\perp} l}{jk_1 Y_1} \frac{\partial}{\partial \rho} G_3 \\ H_\rho = E_\varphi = 0 \end{cases}$	$\begin{cases} {}^{E}_{M}E_\rho = \pm\frac{1}{2} jk_n^{\pm1} Z_n {}^{e}I_0^{\parallel} l \cos\varphi \left(\bar{\bar{I}} \mp \bar{\bar{M}}\right) \frac{\partial^{1\mp1}}{\partial z^{1\mp1}} G_3 \\ {}^{E}_{M}E_\varphi = \mp\frac{1}{2} jk_n^{\pm1} Z_n {}^{e}I_0^{\parallel} l \sin\varphi \left(\bar{\bar{I}} \pm \bar{\bar{M}}\right) \frac{\partial^{1\mp1}}{\partial z^{1\mp1}} G_3 \\ {}^{E}_{M}H_\rho = -\frac{1}{2}{}^{e}I_0^{\parallel} l \sin\varphi \left(\bar{\bar{I}} \pm \bar{\bar{M}}\right) \frac{\partial}{\partial z} G_3 \\ {}^{E}_{M}H_\varphi = -\frac{1}{2}{}^{e}I_0^{\parallel} l \cos\varphi \left(\bar{\bar{I}} \mp \bar{\bar{M}}\right) \frac{\partial}{\partial z} G_3 \end{cases}$

which can be expressed by products of Green's functions and their spatial derivatives (Table I). Consequently, we apply the steepest-descent-path method on the spectral integrals of Table I in order to obtain closed-form expressions for the far-field radiation patterns [1], [2]. The saddle point contribution to the 2D spectral integral yields

$$ {}^{e}_{m}S_r(\theta) = \frac{{}^{e}_{m}\bar{P}_{N+1}}{2\pi r} \left| \left[2j\beta_{N+1} g_{N+1}(z,z') \right]_{k_t = k_{N+1}\sin\theta} \right|^2 \qquad (7) $$

where ${}^{e}_{m}\bar{P}_n = k_n (Z_n)^{\pm1} \left|{}^{e}_{m}I_0\right|^2 / 8$ is the power radiated by the electric or magnetic line source per unit length in an unbounded homogeneous medium of the nth layer material [1].

For the 3D case we substitute the Bessel functions by their integral representation, $J_0(k_t\rho) = \int_0^{\pi} d\psi e^{jk_t\rho\cos\psi}$ [11], and perform successive saddle point evaluation of the resultant double integrals, resulting in the 3D radiation pattern,

$$ {}^{E}_{M}S_r(\theta,\varphi) = \frac{3\,{}^{E}_{M}\xi}{2} \frac{{}^{e}P_{N+1}}{4\pi r^2} \left| \left[2j\beta_{N+1} g_{N+1}(z,z') \right]_{k_t = k_{N+1}\sin\theta} \right|^2 \qquad (8) $$

where ${}^{e}P_n = Z_n \left|{}^{e}I_0 k_n l\right|^2 / (12\pi)$ is the power radiated by an electric dipole in an unbounded homogeneous medium of the nth layer material [1] and the orientation factor, ξ, is given by

$$ {}^{M}\xi^{\perp} = \sin^2\theta, \;\; {}^{E}\xi^{\parallel} = \sin^2\varphi, \;\; {}^{M}\xi^{\parallel} = \cos^2\theta\cos^2\varphi \qquad (9) $$

in consistency with [10]. For molecular optical sources, it is generally assumed that there is no in-plane directional preference for the molecule orientation, i.e., the horizontal dipoles are distributed uniformly in φ [5], [10]. Incoherent averaging of (8) upon the in-plane dipole orientation transforms (9) into

$$ \left\langle {}^{M}\xi^{\perp} \right\rangle_{\varphi} = \sin^2\theta, \;\; \left\langle {}^{E}\xi^{\parallel} \right\rangle_{\varphi} = \frac{1}{2}, \;\; \left\langle {}^{M}\xi^{\parallel} \right\rangle_{\varphi} = \frac{1}{2}\cos^2\theta \qquad (10) $$

III. RESULTS AND DISCUSSION

Equations (7) and (8) express the great similarity between the radiation patterns of the 2D and 3D sources. The heart of all radiation patterns is the 1D Green's function in the observation region, $g_{N+1}(z,z')$, evaluated at the saddle point $k_t = k_{N+1}\sin\theta$. This is analogous to solving the problem in the geometrical optics (GO) approximation, according to which the 1D Green's function accounts for all possible multiple reflections between the layer interfaces of rays which originate at the source and arrive at the observation point following Snell's law (Fermat's principle). Conforming to GO rules, the reflection and transmission coefficients correspond to the polarization of the electromagnetic waves approximated by the rays [1], [2], and vary with the sources according to (4) and (5). This GO picture of (7) and (8) is complemented by the identification of the nominal power radiated by the source in unbounded homogeneous medium, accompanied by the divergence factor, proportional to the surface area of a sphere (3D) or the perimeter of a cylinder (2D) of radius r, and the orientation factor, which takes into account the anisotropic nature of the source radiation (the intrinsic radiation pattern, e.g., no radiation in the direction to which the dipole points).

These observations emphasize that the differences in the angular distribution of the power radiated by the sources, given the unified format (2) of the 1D Green's function, may arise only from the local reflection coefficients (5) or the orientation factors, given by (10) for molecular optical sources. Indeed, in the context of our investigation, these two equations constitute the main result. They imply that as far as the TE-polarized radiation is concerned, the ELS radiation pattern is *identical* to the radiation pattern produced by the optical point dipole, if both are normalized to their maximum. In other words, normalized TE-polarized measurements of realistic devices, containing a combination of HEDs and VEDs, should match theoretical radiation patterns derived for 2D ELSs, as was already observed by us [7].

For the TM-polarized radiation, the relation between the 2D and 3D results is less trivial. However, its analysis is useful, as it highlights the different nature of the two origins of this emission. The VED produces pure TM-polarized emission; in that sense its response is identical to that of the 2D MLS (see

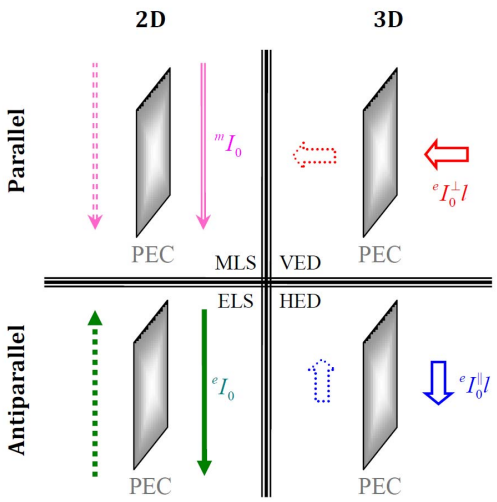

Fig. 2. Images induced by the 2D and 3D sources when placed in front of a perfect electric conductor (PEC). The sources are denoted by solid arrow outlines, and the images by dotted arrow outlines. While the MLS (magenta) and VED (red) induce images aligned parallel to the sources, the ELS (green) and HED (blue) induce antiparallel images.

(5)), with the exception that the intrinsic dipole radiation pattern, proportional to $\sin^2\theta$, must be taken into consideration. On the other hand, the TM-polarized emission originating in the HED is modified with respect to the MLS radiation due to the difference in the orientation of their images: although the local reflection coefficients (5) in both cases follow the TM Fresnel formula (e.g. may exhibit Brewster's angle reflection or coupling to surface plasmons), when images of the MLS are aligned parallel to the source, images of the HED, in the same geometry, would be antiparallel (Fig. 2). Therefore, ${}^{M}\Gamma_n^{\parallel}$ bears a minus sign in (5). The orientation factor in this case is proportional to $\cos^2\theta$, in consistency with the $\pi/2$ orientation shift with respect to the VED.

It is worth noting that the image relations discussed in the previous paragraph may offer a path to directly relate also the TM-polarized 2D results to experimental measurements of arbitrarily oriented dipoles (i.e., modelled by a combination of HEDs and VEDs). As was noted by Flämmich *et al.* [12], the antisymmetry in image alignment of the HEDs and VEDs indicates that when placed in front of a highly reflecting metallic surface, e.g. the cathode in OLEDs, distances which induce constructive interference for the one specie yield destructive interference for the other. This allows, in principle, to design configurations which promote the radiation of only one of the species, based on the location of the sources. This, in turn, would yield TM-polarized radiation dominated by either HED or VED, which can be consequently interpreted in terms of the 2D model, requiring only the consideration of the suitable orientation factor and reflection coefficient.

IV. Conclusion

We have presented a comparison between the radiation patterns produced by 2D electric and magnetic line sources, acting as simplified model sources, and electric 3D point dipoles, representing realistic elementary optical sources, embedded in stratified media. Utilizing a TE/TM decomposition of the horizontal dipole, we were able to show that assuming random in-plane orientation of the incoherent dipoles, the normalized radiation patterns of the 2D electric line source are identical to the TE-polarized emission expected to be measured for the optical sources. For the TM-polarized radiation of the realistic 3D scenario, we have shown that it can be interpreted as originating from a 2D magnetic line source only for the vertical dipole, while for the horizontal dipole, the difference in image orientation should be taken into account. In both cases (vertical and horizontal TM-polarized emission) an orientation factor proportional to the intrinsic radiation pattern of the dipole must be considered.

These results offer an original insight to the contributions of the various realistic 3D sources to the overall radiation, by interpreting them as a combination of modified 2D line sources, generating either pure TE- or pure TM- polarized emission. Furthermore, the exact relations we have derived herein, presenting a unified analytical format for all radiation patterns, indicate in which cases the 2D model is capable of reproducing experimental measurements of physical 3D configurations, and list the necessary modifications, thus enabling a simplified analytical approach to layered media problems.

Acknowledgment

A. E. gratefully acknowledges the support of The Clore Israel Foundation Scholars Programme.

References

[1] L. B. Felsen and N. Marcuvitz, *Radiation and Scattering of Waves*, 1st ed. Englewood Cliffs, N.J.: Prentice-Hall, 1973.
[2] W. C. Chew, *Waves and fields in inhomogeneous media*. New York: Van Nostrand Reinhold, 1990.
[3] R. R. Chance, A. Prock, and R. Silbey, "Molecular fluorescence and energy transfer near interfaces," *Adv. Chem. Phys.*, vol. 37, pp. 1–65, 1978.
[4] K. A. Neyts, "Simulation of light emission from thin-film microcavities," *J. Opt. Soc. Am. A*, vol. 15, no. 4, pp. 962–971, 1998.
[5] M. Furno, R. Meerheim, S. Hofmann, B. Lüssem, and K. Leo, "Efficiency and rate of spontaneous emission in organic electroluminescent devices," *Phys. Rev. B*, vol. 85, p. 115205, Mar 2012.
[6] A. Epstein, N. Tessler, and P. D. Einziger, "The Impact of Spectral and Spatial Exciton Distributions on Optical Emission from Thin-Film Weak-Microcavity Organic Light-Emitting Diodes," *IEEE J. Quantum Electron.*, vol. 46, no. 9, pp. 1388–1395, 2010.
[7] ——, "Analytical extraction of the recombination zone location in organic light-emitting diodes from emission pattern extrema," *Opt. Lett.*, vol. 35, no. 20, pp. 3366–3368, 2010.
[8] I. V. Lindell, "TE/TM decomposition of electromagnetic sources," *IEEE Trans. Antennas Propag.*, vol. 36, no. 10, pp. 1382 –1388, oct 1988.
[9] D. Sokolik, "Power absorption in highly lossy biological tissues: electric dipole excitation," Master's thesis, Technion - Israel Institute of Technology, 2003.
[10] W. Lukosz, "Light emission by magnetic and electric dipoles close to a plane dielectric interface. III. Radiation patterns of dipoles with arbitrary orientation," *J. Opt. Soc. Am.*, vol. 69, no. 11, pp. 1495–1503, Nov. 1979.
[11] R. Piessens, *The Transforms and Applications Handbook*, 2nd ed. Boca Raton: CRC Press, 2000, ch. 2.
[12] M. Flämmich, M. C. Gather, N. Danz, D. Michaelis, A. H. Bräuer, K. Meerholz, and A. Tünnermann, "Orientation of emissive dipoles in OLEDs: Quantitative in situ analysis," *Org. Electron.*, vol. 11, no. 6, 2010.